Supplemental Figure

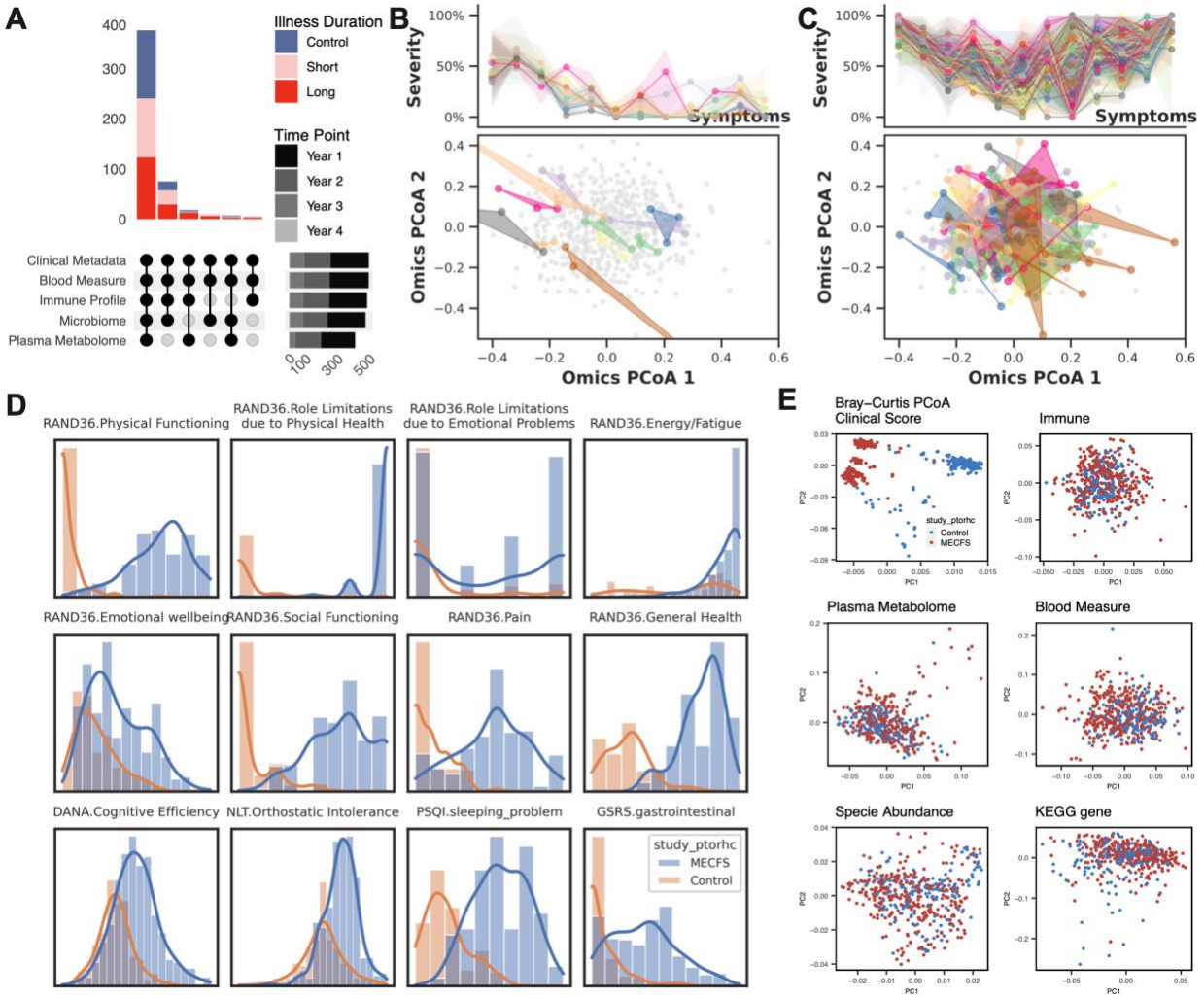

Supplemental Figure 1: Data Pairedness Overview and Heterogeneity in Healthy and Patients. A) Cohort Composition and Data Collection. Over four years, 515 time points were collected: baseline year from all 249 donors (Healthy N=96, ME/CFS N=153); second year from 168 individuals (Healthy N=58, ME/CFS N=110); third year from 94 individuals (Healthy N=13, ME/CFS N=81); fourth year from N=4 ME/CFS patients. Nearly 400 collection points included complete sets of 5 'omics datasets, with others capturing 3-4 'omics profiles. Clinical metadata and blood measures were collected at all 515 points. Immune profiles from PBMCs were recorded at 489 points, microbiome data from stool samples at 479 points, and plasma metabolome data at 414 points. A total of 1,471 biosamples were collected. **B-C) Heterogeneity of B) Healthy Controls and C) All Patients in Symptom Severity and 'Omics Profiles.** Supplemental information for Figure 1B, which shows examples from 20 patients. Variability in symptom severity (top) and 'omics profiles (bottom) for all healthy controls and all patients with 3-4 time points. **D) Distribution of 12 Clinical Symptoms in ME/CFS and Control.** Density plots compare the distributions of 12 clinical scores between control (blue) and ME/CFS patients (orange) with the y-axis representing severity (scaled from 0% to 100%). Clinical scores include RAND36 subscales (e.g., Physical Functioning, Emotional Wellbeing), Cognitive Efficiency from

the DANA test, Orthostatic Intolerance from the NLT test, Sleep Problems from the PSQI questionnaire, and Gastrointestinal Symptoms from the GSRS questionnaire. **E) Principal Coordinates Analysis (PCoA) of each 'Omics.** PCoA based on Bray-Curtis distance for clinical scores, immune profiles, plasma metabolome, blood measures, species abundance, and KEGG gene data. Control samples (blue) and ME/CFS patients (red) show distinct clustering. Here, except for the clinical scores, controls are indistinguishable from patients, highlighting the difficulty of building classification models. **Abbreviations:** ME/CFS, Myalgic Encephalomyelitis/Chronic Fatigue Syndrome; PCoA, Principal Coordinates Analysis; RAND36, 36-Item Short Form Health Survey; DANA, DANA Brain Vital; NLT, NASA Lean Test; PSQI, Pittsburgh Sleep Quality Index; GSRS, Gastrointestinal Symptom Rating Scale; KEGG, Kyoto Encyclopedia of Genes and Genomes. **Related to:** Figure 1-2.

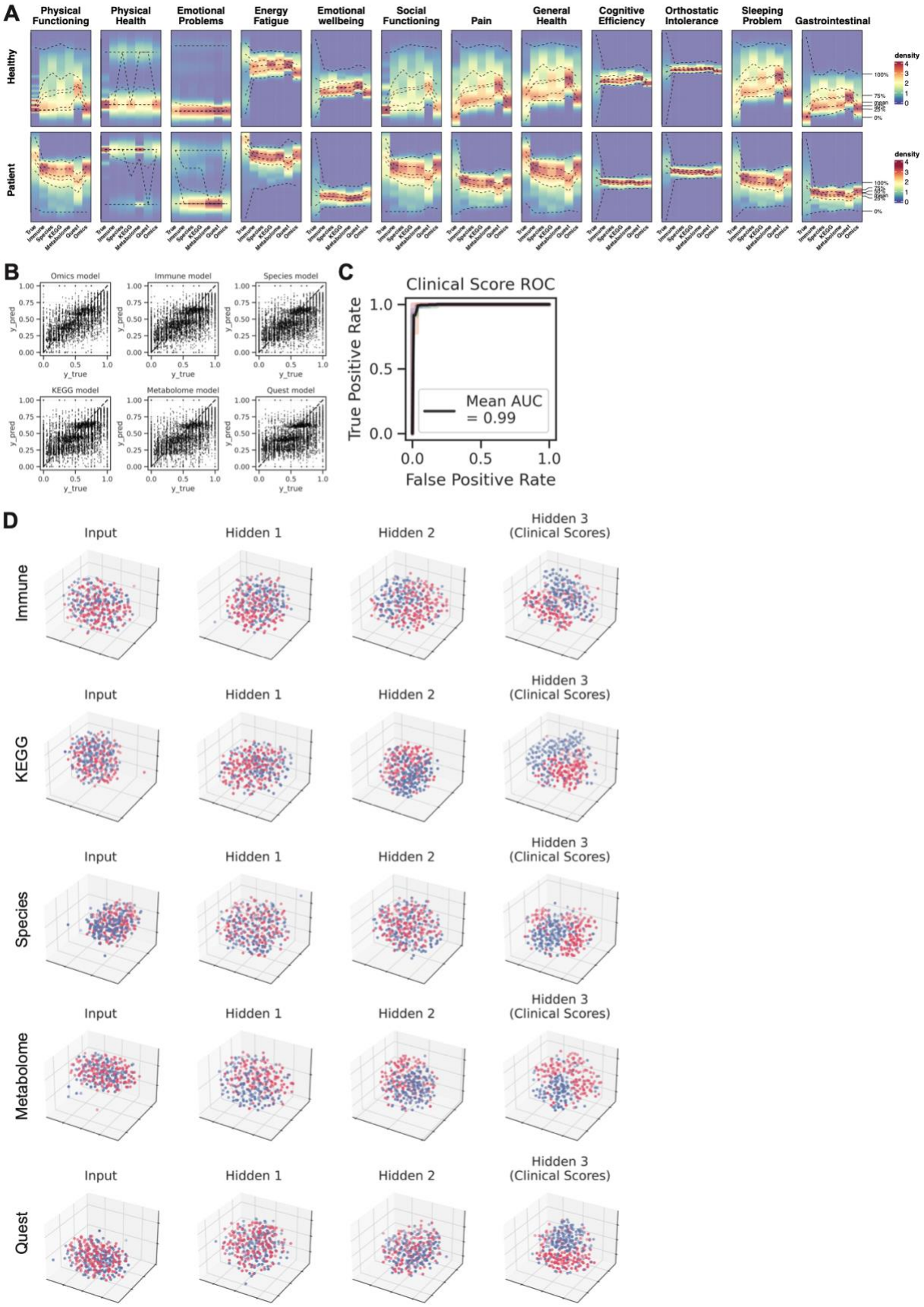

1104

Supplemental Figure 2: BioMapAI's Performance at Clinical Score Reconstruction and Disease Classification. A) Density map of True vs. Predicted Clinical Scores. Supplemental information for Figure 2B, which shows three examples. Here, the full set of 12 clinical scores compares the true score, y (Column 1), against BioMapAI's predictions generated from different 'omics profiles – $\hat{y}_{immune}$, $\hat{y}_{species}$, $\hat{y}_{KEGG}$, $\hat{y}_{metabolome}$, $\hat{y}_{quest}$, $\hat{y}_{omics}$ (Columns 2-7). **B) Scatter Plot of True vs. Predicted Clinical Scores.** Scatter plots display the relationship between true clinical scores (x-axis) and predicted clinical scores (y-axis) for six different models: Omics, Immune, Species, KEGG, Metabolome, and Quest Labs. Each plot demonstrates the clinical score prediction accuracy for each model. **C) ROC Curve for Disease Classification with Original Clinical Scores.** The Receiver Operating Characteristic (ROC) curve evaluates the performance of disease classification using the original 12 clinical scores. The mean Area Under the Curve (AUC) is 0.99, indicating high prediction accuracy, which aligns with the clinical diagnosis of ME/CFS based on key symptoms. **D) 3D t-SNE Visualization of Hidden Layers.** 3D t-SNE plots show how BioMapAI progressively distinguishes disease from control across hidden layers for five trained 'omics models: Immune, KEGG, Species, Metabolome, and Quest Labs. Each plot uses the first three principal components to show the spatial distribution of control samples (blue) and ME/CFS patients (red). The progression from the input layer (mixed groups) to Hidden Layer 3 (fully separated groups) illustrates how BioMapAI progressively learns to separate ME/CFS from healthy controls. **Abbreviations:** ROC, Receiver Operating Characteristic; AUC, Area Under the Curve; t-SNE, t-Distributed Stochastic Neighbor Embedding; PCs, Principal Components; y, True Score; $\hat{y}$, Predicted Score. **Related to:** Figure 2.

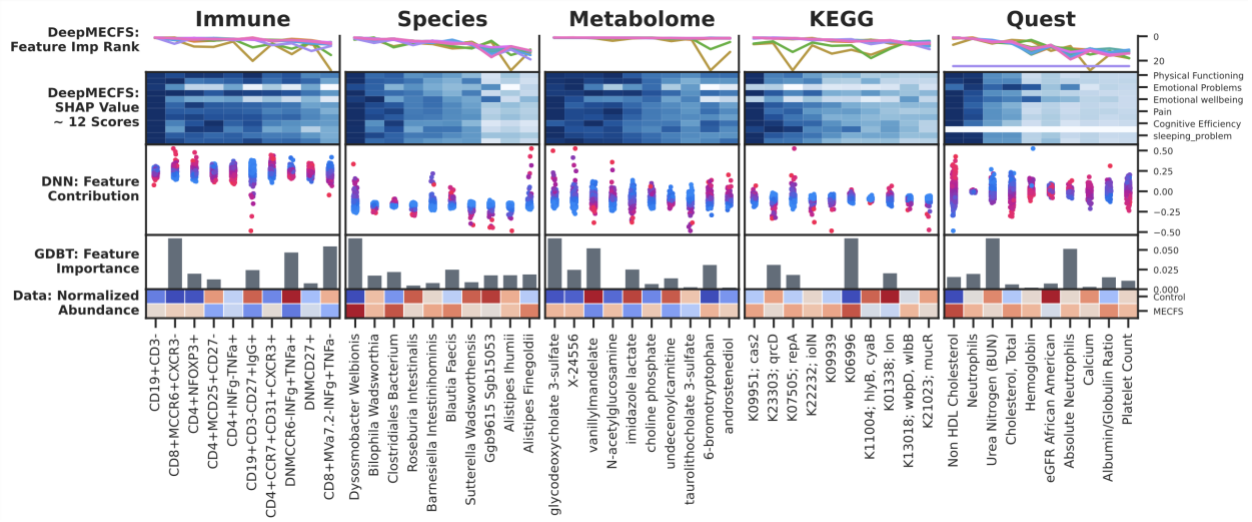

Supplemental Figure 3: Disease-Specific Biomarkers - Top 10 Biomarkers Shared across Clinical Symptoms and Multiple Models. Through the top 30 high-ranking features for each score, we discovered that the most critical features for all 12 symptoms were largely shared and consistently validated across ML and DL models, particularly the foremost 10. Here, this multi-panel figure presents the top 10 most significant features identified by BioMapAI across five 'omics profiles, highlighting their importance in predicting clinical symptoms and diagnostic outcomes across BioMapAI, DNN, and GBDT models, along with their data prevalence. Each vertical section represents one 'omics profile, with columns of biomarkers ordered by average feature importance from right to left. From top to bottom: *1. Feature Importance Ranking in BioMapAI.* Lines depict the rank of feature importance for each clinical score, color-coded by the 12 clinical scores. Consistency among the top 5 features suggests they are shared disease biomarkers crucial for all clinical symptoms; *2. Heatmap of SHAP Values from BioMapAI.* This heatmap shows averaged SHAP values with the 12 scores on the rows and the top 10 features in the columns. Darker colors indicate a stronger impact on the model's output; *3. Swarm Plot of SHAP Values from DNN.* This plot represents the distribution of feature contributions from DNN, which is structurally similar to BioMapAI but omits the third hidden layer (Z^3). SHAP values are plotted vertically, ranging from negative to positive, showing each feature's influence on prediction outcomes. Points represent individual samples, with color gradients denoting actual feature values. For instance, *Dysosmobacteria welbionis*, identified as the most critical species, shows that greater species relative abundance correlates with a higher likelihood of disease prediction; *4. Bar Graphs of Feature Importance in GBDT*. GBDT is another machine learning model used for comparison. Each bar's height indicates a feature's significance within the GBDT model, providing another perspective on the predictive relevance of each biomarker; *5. Heatmap of Normalized Raw Abundance Data.* This heatmap compares biomarker prevalence between healthy and disease states, with colors representing z-scored abundance values, highlighting biomarker differences between groups. **Abbreviations:** DNN: Here refer to our deep Learning model without the hidden 3, 'spread out' layer; GBDT: Gradient Boosting Decision Tree; SHAP: SHapley Additive exPlanations. **Supporting Materials:** Supplemental Table 5. **Related to:** Figure 3.

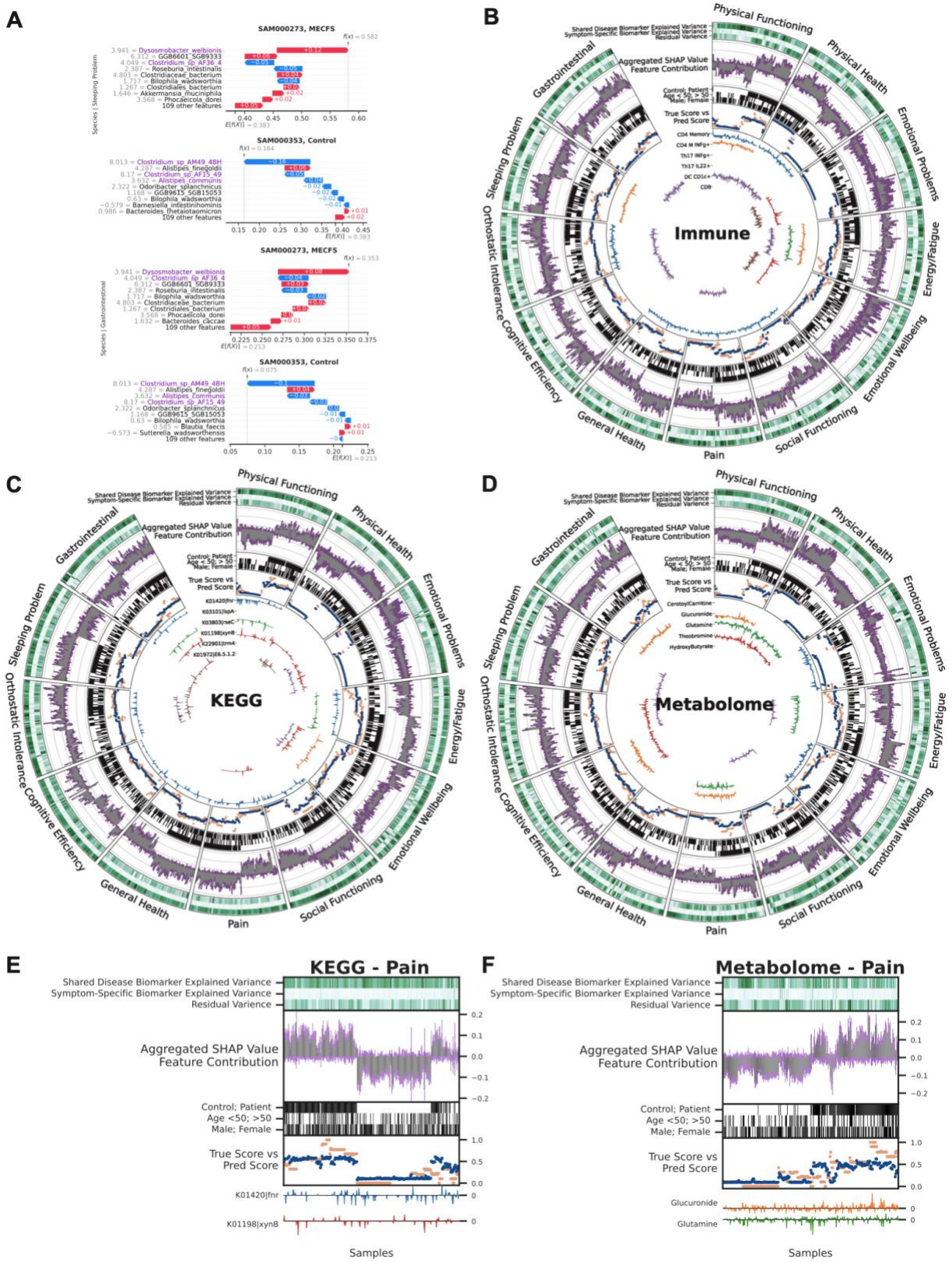

Supplemental Figure 4: Symptom-Specific Biomarkers - Immune, KEGG and Metabolome Models. By linking 'omics profiles to clinical symptoms, BioMapAI identified unique symptom-

specific biomarkers in addition to disease-specific biomarkers (Supplemental Figure 3). Each 'omics has a circularized diagram (Figure 3A, Supplemental Figure 4B-D) to display how BioMapAI use this 'omics profile to predict 12 clinical symptoms and to discuss the contribution of disease- and symptom-specific biomarkers. Detailed correlation between symptom-specific biomarkers and their corresponding symptoms is in Supplemental Figure 5. **A) Examples of Sleeping Problem-Specific Species' and Gastrointestinal-Specific Species' Contributions.** Supplemental information for Figure 3D, which shows the contribution of pain-specific species. **B-D) Circularized Diagram for Immune, KEGG and Metabolome Models.** Supplemental information for Figure 3A, which shows the species model. **E-F) Zoomed Segment for Pain in KEGG and Metabolome Model.** Supplemental information for Figure 3B, which shows the zoomed segment for pain in the species and immune models. **Abbreviations and Supporting Materials:** Supplemental Figure 5. **Related to:** Figure 3.

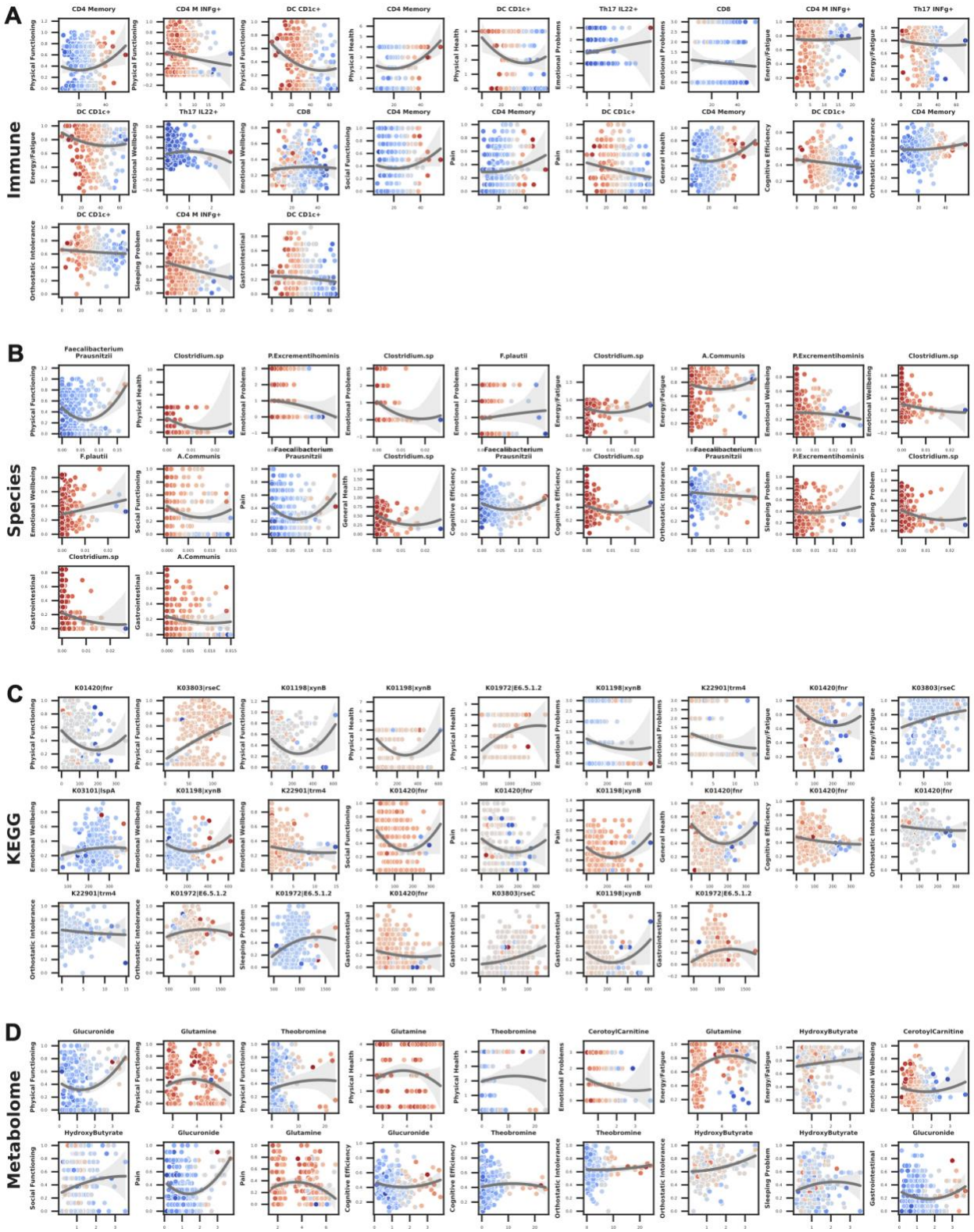

Supplemental Figure 5: Symptom-Specific Biomarkers - Different Correlation Patterns of Biomarkers to Symptom. Supplemental information for Figure 3C, which shows six pain biomarkers from multiple models. Here for each 'omics, we plotted the correlation of symptom-

specific biomarkers (x-axis) to its related symptom (y-axis), colored by SHAP value (contribution to the symptom). **Abbreviations:** CD4, Cluster of Differentiation 4; CD8, Cluster of Differentiation 8; IFNg, Interferon Gamma; DC, Dendritic Cells; MAIT, Mucosal-Associated Invariant T; Th17, T helper 17 cells; CD4+ TCM, CD4+ Central Memory T cells; DC CD1c+ mBtp+, Dendritic Cells expressing CD1c+ and myelin basic protein; DC CD1c+ mHsp, Dendritic Cells expressing CD1c+ and heat shock protein; CD4+ TEM, CD4+ Effector Memory T cells; CD4+ Th17 rfx4+, CD4+ T helper 17 cells expressing RFX4; *F. prausnitzii, Faecalibacterium prausnitzii; A. communis, Akkermansia communis*; NAD, Nicotinamide Adenine Dinucleotide. **Related to:** Figure 3.

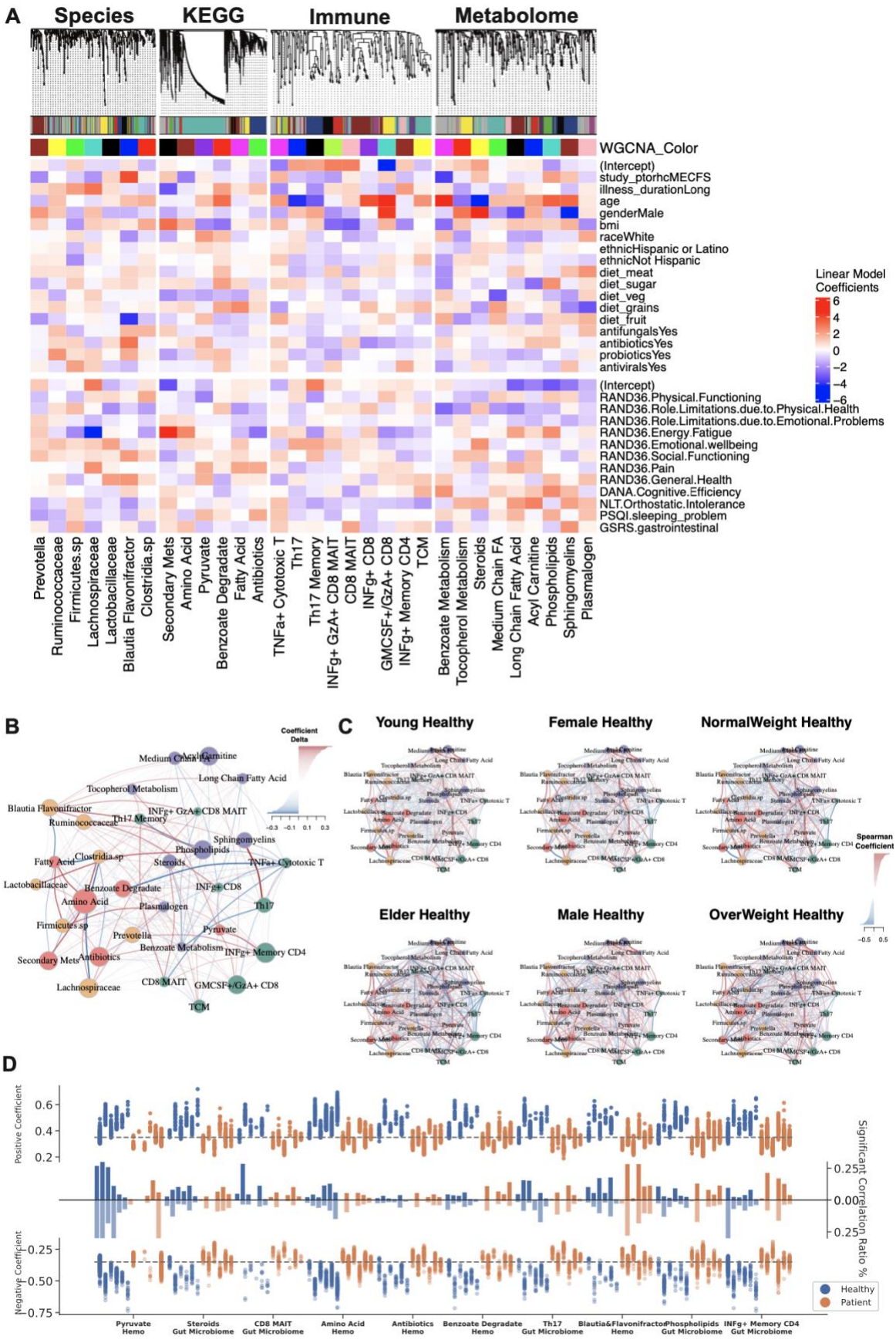

Supplemental Figure 6: 'Omics WGCNA Modules and Host-Microbiome Network. A) Correlation of WGCNA Modules with Clinical Metadata. Weighted Gene Co-expression Network Analysis (WGCNA) was used to identify co-expression modules for each 'omics layer: species, KEGG, immune, and metabolome. The top dendrograms show hierarchical clustering of 'omics features, with modules identified. The bottom heatmap shows the relationship of module eigengenes (colored as per dendrogram) with clinical metadata – including demographic information and environmental factors - and 12 clinical scores. General linear models were used to determine the primary clinical drivers for each module, with the color gradient representing the coefficients (red = positive, blue = negative). Microbial modules were influenced by disease presence and energy-fatigue levels, while metabolome and immune modules correlated with age and gender. **B-C) Microbiome-Immune-Metabolome Network in B) Patient and C) Healthy Subgroups.** Supplemental information for Figure 4A (Healthy Network) and 4B (Patient Subgroups). Figure 4A is the healthy network; here, Supplemental Figure 6B presented the shifted correlations in all patients. Figure 4B represented the network in patient subgroups; here, Supplemental Figure 6C is the corresponding healthy counterpart, for example, female patients were compared with female controls to exclude gender influences. **D) Differences in Host-Microbiome Correlations between Healthy and Patient Subgroups.** Selected host-microbiome module pairs are grouped on the x-axis (e.g., pyruvate to blood modules, steroids to gut microbiome). Significant positive and negative correlations (top and bottom y-axis) of module members pairs are shown as dots for each subgroup (blue = healthy, orange = patient) (Spearman, adjusted $p < 0.05$), from left to right: Young, Elder, Female, Male, NormalWeight, OverWeight Healthy and Young, Elder, Female, Male, NormalWeight, OverWeight Patient. The middle bars represent the total count of associations. This panel highlights the shifts in host-microbiome networks from health to disease, for example, in patients, the loss of pyruvate to host blood modules correlation and the increase of INFg+ CD4 memory correlation with gut microbiome. **Abbreviations:** WGCNA, Weighted Gene Co-expression Network Analysis; AA, Amino Acids; SCFA, Short-Chain Fatty Acids; IL, Interleukin; GM-CSF, Granulocyte-Macrophage Colony-Stimulating Factor. **Related to**: Figure 4.